

# Paper III

Sølve Selstø, Morten Førre, Jan Petter Hansen and Lars Bojer Madsen

**Strong Orientation Effects in Ionization of  $\text{H}_2^+$  by Short, Intense, High-Frequency  
Light Pulses**

*Physical Review Letters* **95**, 093002 (2005).

**Strong Orientation Effects in Ionization of  $\text{H}_2^+$  by Short, Intense, High-Frequency Light Pulses**S. Selstø,<sup>1</sup> M. Førre,<sup>1</sup> J. P. Hansen,<sup>1</sup> and L. B. Madsen<sup>2</sup><sup>1</sup>*Department of Physics and Technology, University of Bergen, N-5007 Bergen, Norway*<sup>2</sup>*Department of Physics and Astronomy, Aarhus University, DK-8000 Aarhus C, Denmark*

(Received 16 February 2005; published 26 August 2005)

We present three-dimensional time-dependent calculations of ionization of arbitrarily spatially oriented  $\text{H}_2^+$  by attosecond, intense, high-frequency laser fields. The ionization probability shows a strong dependence on both the internuclear distance and the relative orientation between the laser field and the internuclear axis. The physical features are explained in terms of two-center interference effects.

DOI: 10.1103/PhysRevLett.95.093002

PACS numbers: 33.80.Rv

The ionization dynamics of one- and two-electron processes in diatomic molecules in short, strong laser fields are at present under intense experimental investigation [1–3]. A part of these investigations also focus on the sensitivity of such processes to molecular orientation with respect to the light polarization [4]. This is again related to the ultimate goal of controlling chemical reactions by aligning the reactive molecules with respect to each other prior to the intermolecular interaction [5].

From a theoretical viewpoint such studies are extremely complex in the strong-field regime and have been of continuous interest for nearly two decades (for reviews, see, e.g., [6]). In general, only results based on approximate theories such as the molecular strong-field approximation [7,8] and tunneling [9] models have been applied to calculate effects related to molecular orientation with respect to the light polarization vector. Such approximate theories are, however, often gauge dependent [8,10] and limited in their applicability to describe complex processes. The “slowness” of past and present computers, combined with computational challenges related to Coulombic multicenter problems, has restricted exact theoretical calculations including both electronic and nuclear degrees of freedom to cases where the internuclear axis is parallel with the linear polarization direction [11,12] or models of reduced dimensionality [13–15]. These studies have given insight into the fascinating interplay between electronic and nuclear degrees of freedom, phenomena which at present are beyond reach of full-dimensional computations.

In this Letter, we present the first full time-dependent three-dimensional calculations for the electronic degrees of freedom in  $\text{H}_2^+$  exposed to a short, strong, attosecond laser pulse. The purpose is to follow the behavior of the system with internuclear distance and in particular to display the dependence of the dynamics on the angle between the internuclear axis and the linear polarization of the field. Calculations are performed for 6 cycle pulses with  $\omega = 2$  a.u. (23 nm) central frequency. This corresponds to pulse durations about 450 asec, which have already been demonstrated [16]. The ionization probability for  $\text{H}(2p)$  atoms

exposed to similar light pulses [17] showed a factor 10 stronger modulation with changing orientation than what was measured with femtosecond pulses [4]. Similar effects in diatomic molecules can thus indicate that attosecond pulses may be sensitive probes of the internal nuclear quantum state as well as its orientation. The calculations indeed display that the ionization probability depends strongly on these parameters. Specifically, it is found that for polarization parallel with the internuclear axis the ionization probability oscillates strongly as the internuclear separation increases, whereas these oscillations are absent at perpendicular polarization. Consequently, a strong dependence on the angle between the internuclear axis and the polarization direction is observed. Atomic units ( $\hbar = m_e = e = 1$ ) are applied throughout.

As the nuclear vibrational period is approximately  $10^3$  times larger than the pulse duration, the nuclear degrees of freedom can be considered frozen during the attosecond pulse. Postpulse interplay between nuclear and electronic degrees of freedom, which are important for weaker fields, is also found to be unimportant here as direct electronic ionization dominates.

The vector potential for the light pulse is given by

$$\mathbf{A}(t) = \frac{E_0}{\omega} \sin^2\left(\frac{\pi}{T}t\right) \sin(\omega t + \phi) \mathbf{u}_p, \quad (1)$$

where  $\mathbf{u}_p$  is a unit vector defining the orientation of the linearly polarized field with maximum amplitude  $E_0$ , and  $\phi$  is the carrier envelope phase. The validity of the dipole approximation was investigated in detail very recently for the present intensity and frequency regime, and was found to be well-justified for ionization [18]. The vector potential determines the electric field,  $\mathbf{E}(t) = -\partial_t \mathbf{A}(t)$ , and the translation,  $\boldsymbol{\alpha}(t) = \int_0^t \mathbf{A}(t') dt'$ , which enter the length  $H_I$  and the Kramers-Henneberger  $H_{\text{KH}}$  form [19] of the interaction Hamiltonian, respectively,

$$H_I = \frac{p^2}{2} - \frac{1}{|\mathbf{r} + \mathbf{R}/2|} - \frac{1}{|\mathbf{r} - \mathbf{R}/2|} + \mathbf{E}(t) \cdot \mathbf{r}, \quad (2)$$

$$H_{\text{KH}} = \frac{p^2}{2} - \frac{1}{|\mathbf{r} + \mathbf{R}/2 + \boldsymbol{\alpha}(t)|} - \frac{1}{|\mathbf{r} - \mathbf{R}/2 + \boldsymbol{\alpha}(t)|}, \quad (3)$$

with  $\mathbf{R}$  the internuclear distance. Both versions of the Hamiltonian have been applied here to secure invariant results.

For fixed nuclei, we solve the time-dependent Schrödinger equation numerically based on a split-step operator approximation on a spherical grid. The method was described in detail elsewhere [20,21]. It should be noted, however, that this is its first application to a molecular system. Converged results have been obtained using a basis of spherical harmonics including up to  $l_{\text{max}} = 15$  as shown in the upper panel of Fig. 1.

After the pulse a fraction of the wave function has been removed by the absorber, enabling us to find the ionization probability. However, since excitation is found to be a minor channel at moderate intensities, the ionization probability can be calculated as  $P_{\text{ion}} = 1 - |\langle \Psi_0 | \Psi(T) \rangle|^2$  in these cases. It is found that the ionization probability is unaltered by a change in the carrier envelope phase  $\phi$ .

The ionization probability versus internuclear separation and electric field strength is displayed in Fig. 1 for field polarization parallel with the internuclear axis. Two striking maxima are observed, one for small internuclear separation,  $R \sim 1$  a.u., and another for  $R \sim 3$  a.u.. When the field strength is further increased, the ionization probability decreases; i.e., the molecule is partly stabilized in the intense field. This rather counterintuitive mechanism has

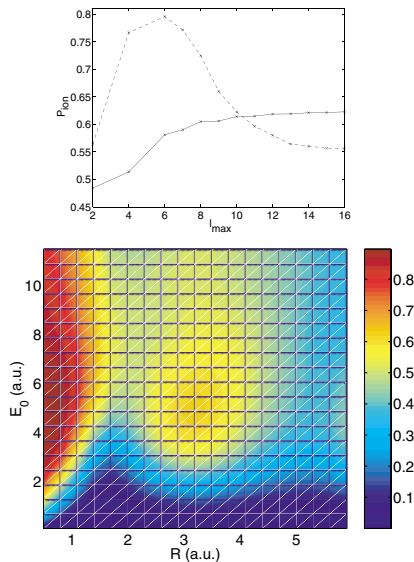


FIG. 1 (color). Lower panel: Ionization probability in the parallel geometry ( $\theta = 0^\circ$ ) as a function of the internuclear separation  $R$  and the electric field strength  $E_0$  with  $\omega = 2$  a.u. and  $T = 6\pi$  a.u.. Upper panel: Convergence of the ionization probability versus  $l_{\text{max}}$  for  $E_0 = 4$  a.u. and  $R = 3$  a.u. (solid curve) and for  $E_0 = 8$  a.u. and  $R = 4$  a.u. (dashed curve).

been studied in detail for atoms [22]. What happens is that for increasing intensity the probabilities for single-photon and multiphoton ionization increase to a maximum value, followed by a steady decrease to zero. In this strong-field limit the Hamiltonian effectively becomes time independent in the Kramers-Henneberger picture, and shakeoff ionization dynamics, i.e., direct projection from the initial field-free state on the continuum eigenstates of the Kramers-Henneberger Hamiltonian, becomes the dominating ionization mechanism. At the ground state equilibrium distance,  $R \sim 2$  a.u. and  $R \sim 5$  a.u., the ionization probability is significantly smaller than the peak regions at  $R \sim 1$  a.u. and  $R \sim 3$  a.u., indicating a strong dynamic self-interference effects of the electronic charge clouds associated with each scattering center.

From Fig. 1 we see that the variation in the ionization signal is most pronounced for  $E_0 \sim 3$  a.u.. At this field strength, Fig. 2 exposes the ionization probability as a function of internuclear separation and as a function of the angle  $\theta$  between the internuclear axis and the polarization direction of the field. An oscillatory behavior of the ionization probability in the parallel geometry ( $\theta = 0^\circ$ ) is seen. As  $\theta$  increases, the oscillations gradually decrease, and in the perpendicular geometry ( $\theta = 90^\circ$ ), the ionization probability drops monotonically with  $R$ . In the figure, we also observe opposite functional dependence with  $\theta$ : At  $R \sim 2$  a.u. the ionization probability increases with  $\theta$ , while at  $R \sim 3$  a.u. it decreases.

We now turn to the detailed dynamics underlying the phenomena observed in Fig. 2. Figure 3 shows snapshots of the wave function in the  $xz$  plane at various times for parallel and perpendicular polarization (the molecule has its internuclear axis directed along the  $z$  axis). In general, the photoelectron is ionized in the directions of the field. For  $\theta = 0^\circ$  the initial charge cloud is partly dragged back and forth along the field, and this gives rise to a strong interference between various momentum components of the wave function and hence the oscillatory dependence with  $R$  in Fig. 1. This effect is absent at  $\theta = 90^\circ$  where the two atomlike charge clouds pertaining to each nucleus

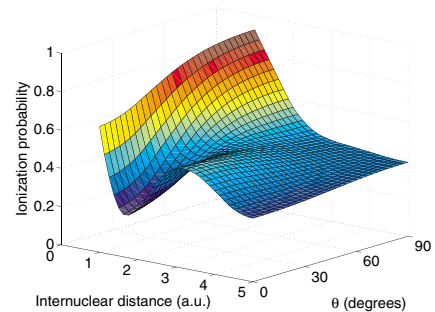


FIG. 2 (color online). Ionization probability as a function of the internuclear separation  $R$  and of the angle  $\theta$  between the polarization direction and the internuclear axis with  $\omega = 2$  a.u.,  $E_0 = 3$  a.u., and  $T = 6\pi$  a.u..

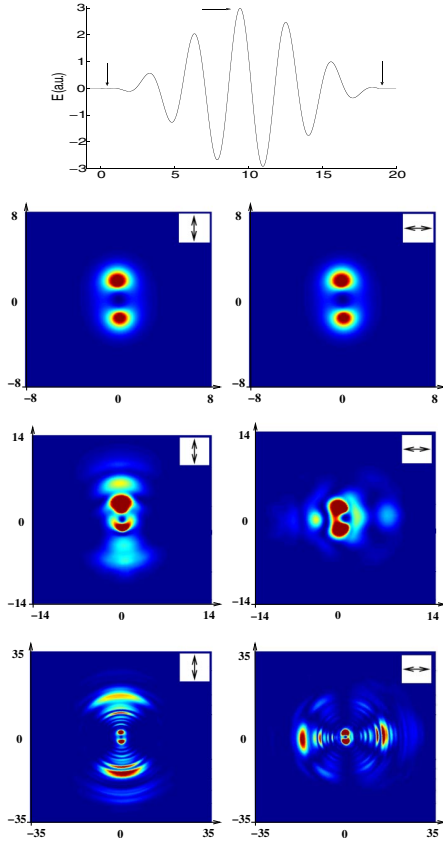


FIG. 3 (color online). Upper panel: The electric field  $E(t)$  of duration  $T = 6\pi$  a.u. (450 asec) and frequency  $\omega = 2$  a.u.. The arrows indicate the instants of time at which the snapshots of the lower part of the figure are made. Snapshots of the wave function in the  $xz$  plane at times corresponding to the beginning (top row), the middle (middle row), and the end (bottom row) of the pulse for parallel (left column) and perpendicular (right column) orientation. In all cases the internuclear separation is  $R = 3$  a.u.. Both the polarization direction and the internuclear axis lie in the  $xz$  plane.

oscillate in phase back and forth with the electric field. In the lower right panel, secondary intensity maxima appear at  $30^\circ$  and  $150^\circ$  with respect to the internuclear axis.

The following simple ansatz offers an explanation of the oscillations at  $\theta = 0^\circ$  and their absence at  $\theta = 90^\circ$ : Assume that the outgoing wave is a superposition of two outgoing spherical waves, one from each of the scattering centers,

$$\psi_{\text{out}} = f_1(\Omega_1) \frac{e^{ik|\mathbf{r}+\mathbf{R}/2|}}{|\mathbf{r}+\mathbf{R}/2|} + f_2(\Omega_2) \frac{e^{ik|\mathbf{r}-\mathbf{R}/2|}}{|\mathbf{r}-\mathbf{R}/2|}. \quad (4)$$

If we take the two scattering amplitudes to be equal,  $f_1(\Omega_1) = f_2(\Omega_2)$ , the differential ionization probability can be brought to the form

$$\frac{dP_{\text{ion}}}{d\Omega} \propto |f_1(\Omega)|^2 [1 + \cos(k\hat{\mathbf{r}} \cdot \mathbf{R})] \quad (5)$$

for  $r \gg R$ . As seen from Fig. 3, the main part of the outgoing wave follows the orientation of the field. Hence we expect that for parallel polarization the main contributions will be for  $\hat{\mathbf{r}}$  parallel to  $\mathbf{R}$ . This gives rise to oscillations in  $R$  with wave number  $k \approx \sqrt{2(\omega - I_p)}$  for one photon processes, where  $I_p(R)$  is the ionization potential. The periodicity is seen to be consistent with the results in Figs. 1 and 2, and we have also confirmed these findings for other values of  $\omega$ . The absence of oscillations in the case of perpendicular polarization is understood accordingly: The wave is sent out mainly in the direction given by  $\theta = 90^\circ$ , and since the outgoing waves will have no phase difference due to the separation of the scattering centers in this direction, this interference will not cause any  $R$  dependence in the ionization probability ( $\hat{\mathbf{r}} \cdot \mathbf{R} = 0$ ). The monotonic decrease in  $P_{\text{ion}}$  with  $R$  at  $\theta = 90^\circ$  is due to the decrease in the ionization potential which leads to an effective higher final state electronic momentum.

The angular distribution of the ionization probability can be calculated from the time integral of the radial current density through the solid angle element  $d\Omega$  at a chosen distance  $a$  from the origin

$$\frac{dP_{\text{ion}}}{d\Omega} = \int_0^\infty dt \mathbf{j}(a, t) \cdot \hat{\mathbf{r}} = \int_0^\infty dt \text{Im} \left( \Psi^* \frac{\partial \Psi}{\partial r} \Big|_a \right), \quad (6)$$

where the distance  $a$  is chosen large enough to exclude contribution to the current from the quiver motion of an electron close to the nucleus and small enough to avoid effects induced by the absorber.

The application of this procedure to the outgoing waves of the lower panels of Fig. 3 results in the intensity spectra of Fig. 4. In this figure, the predictions of the above two-center scattering model is also shown based on the following assumptions: Since the ground state of  $\text{H}_2^+$  has a dominating  $s$ -wave configuration, we may safely assume that a central part of the photoelectron is represented by a  $p$  wave when one photon ionization is the dominating process [23]. Since the scattering amplitude should have its maximum value in the direction of the polarization, we further assume that  $f_1 \propto Y_{10}$  and  $f_1 \propto Y_{1x} = (Y_{1-1} - Y_{11})/\sqrt{2}$  for parallel and perpendicular polarization, respectively. We see that the existence of the local maxima at intermediate angles is fully described based on this model. A small asymmetry is visible in the differential full numerical calculation. This is due to the relatively low number of optical cycles. The angular distribution is slightly modified by a change in the carrier envelope phase  $\phi$ . For a smaller number of cycles, it is well known that the asymmetry can be very large [24]. It is also interesting to note that in a very recent calculation of high harmonic generation (HHG) in a reduced model with respect to the electronic degrees of freedom, this interference phenomenon giving rise to local maxima does not occur [25]. In that work it is pointed out that orientational effects are very important for HHG.

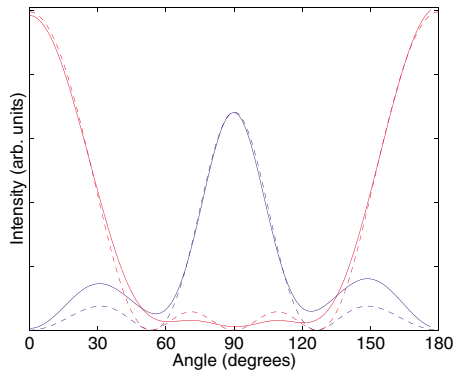


FIG. 4 (color). Angular photoelectron spectra in the scattering plane for parallel (red lines) and perpendicular (blue lines) geometry as a function of the polar angle for a 6 cycle field with  $E_0 = 3$  a.u. and  $\omega = 2$  a.u.. The solid curve is obtained using Eq. (6) and the dashed one by using Eq. (5) with a “best fit” obtained for a wave number of  $k = 1.77$  a.u.. The carrier envelope phase  $\phi$  is here zero. In all cases, the angle denotes the direction of the outgoing electron with respect to the internuclear axis.

In conclusion, fully nonperturbational calculations of the ionization dynamics of  $H_2^+$  molecules in intense attosecond light pulses have been carried out. Very strong orientation effects have been found, demonstrating that, in order to obtain a full understanding of the molecular ionization dynamics, all three electronic degrees of freedom must be included. The geometrical effects are determined by interference related to double-center scattering and the distinct features in the electron spectra show that intense attosecond pulses can resolve the instantaneous vibrational and orientational quantum state of diatomic molecules.

It is a pleasure to thank Thomas K. Kjeldsen for useful discussions and for critically reading the manuscript. The present research was supported by the Norwegian Research Council through the NANOMAT program and the Nordic Research Board NordForsk and by the Danish Natural Science Research Council.

[1] E. Eremina, X. Liu, H. Rottke, W. Sandner, M. G. Schätzel, A. Dreischuh, G. G. Paulus, H. Walther, R. Moshhammer, and J. Ullrich, *Phys. Rev. Lett.* **92**, 173001 (2004).  
 [2] A. S. Alnaser, X. M. Tong, T. Osipov, S. Voss, C. M. Maharjan, P. Ranitovic, B. Ulrich, B. Shan, Z. Chang, C. D. Lin, and C. L. Cocke, *Phys. Rev. Lett.* **93**, 183202 (2004).

[3] X. Urbain, B. Fabre, E. M. Staicu-Casagrande, N. de Ruelle, V. M. Andrianarijaona, J. Jureta, J. H. Posthumus, A. Saenz, E. Baldit, and C. Cornaggia, *Phys. Rev. Lett.* **92**, 163004 (2004).  
 [4] I. V. Litvinyuk, K. F. Lee, P. W. Dooley, D. M. Rayner, D. M. Villeneuve, and P. B. Corkum, *Phys. Rev. Lett.* **90**, 233003 (2003).  
 [5] C. Z. Bisgaard, M. D. Poulsen, E. Peronne, S. S. Viftrup, and H. Stapelfeldt, *Phys. Rev. Lett.* **92**, 173004 (2004).  
 [6] *Molecules in Laser Fields*, edited by A. D. Bandrauk (Marcel Dekker, New York, 1994); *Molecules and Clusters in Intense Laser Fields*, edited by J. H. Posthumus (Cambridge University Press, Cambridge, 2001).  
 [7] J. Muth-Böhm, A. Becker, and F. H. M. Faisal, *Phys. Rev. Lett.* **85**, 2280 (2000).  
 [8] T. K. Kjeldsen and L. B. Madsen, *J. Phys. B* **37**, 2033 (2004).  
 [9] Z. X. Zhao, X. M. Tong, and C. D. Lin, *Phys. Rev. A* **67**, 043404 (2003).  
 [10] L. B. Madsen, *Phys. Rev. A* **65**, 053417 (2002).  
 [11] D. Dundas, *Phys. Rev. A* **65**, 023408 (2002).  
 [12] M. Plummer and J. McCann, *J. Phys. B* **30**, L401 (1997).  
 [13] B. Rotenberg, R. Taïeb, V. Veniard, and A. Maquet, *J. Phys. B* **35**, L397 (2002).  
 [14] B. Feuerstein and U. Thumm, *Phys. Rev. A* **67**, 063408 (2003).  
 [15] V. Roudnev, B. D. Esry, and I. Ben-Itzhak, *Phys. Rev. Lett.* **93**, 163601 (2004).  
 [16] A. Baltuska, T. Udem, M. Uiberacker, M. Hentschel, E. Goulielmakis, C. Gohle, R. Holzwarth, V. S. Yakovlev, T. W. H. A. Scrinzi, and F. Krausz, *Nature (London)* **421**, 611 (2003); M. Drescher, M. Hentschel, R. Kienberger, M. Uiberacker, V. Yakovlev, A. Scrinzi, T. Westerwalbasloh, U. Kleineberg, U. Heinzmann, and F. Krausz, *Nature (London)* **419**, 803 (2002).  
 [17] T. Birkeland, M. Førre, J. P. Hansen, and S. Selstø, *J. Phys. B* **37**, 4205 (2004).  
 [18] M. Førre, J. P. Hansen, S. Selstø, and L. B. Madsen, *Phys. Rev. Lett.* **95**, 043601 (2005).  
 [19] W. Pauli and M. Fierz, *Nuovo Cimento* **15**, 167 (1938); H. A. Kramers, *Collected Scientific Papers* (North-Holland, Amsterdam, 1956), p. 866; W. C. Henneberger, *Phys. Rev. Lett.* **21**, 838 (1968).  
 [20] M. R. Hermann and J. A. Fleck, Jr., *Phys. Rev. A* **38**, 6000 (1988).  
 [21] J. P. Hansen, T. Sjørevik, and L. B. Madsen, *Phys. Rev. A* **68**, 031401(R) (2003).  
 [22] M. Gavrilu, *J. Phys. B* **35**, R147 (2002).  
 [23] P. Lambropoulos, P. Maragakis, and Jian Zhang, *Phys. Rep.* **305**, 203 (1998).  
 [24] H. M. Nilsen and J. P. Hansen, *Phys. Rev. A* **63**, 011405(R) (2001).  
 [25] M. Lein, *Phys. Rev. Lett.* **94**, 053004 (2005).